LEGIBILITY NOTICE

A major purpose of the Technical Information Center is to provide the broadest dissemination possible of information contained in DOE's Research and Development Reports to business, industry, the academic community, and federal, state and local governments.

Although a small portion of this report is not reproducible, it is being made available to expedite the availability of information on the research discussed herein.

Los Alamos National Laboratory is operated by the University of California for the United States Department of Energy under contract W-7405-ENG-36

LA-UR--89-1636

DE89 012612

TITLE: AXIALLY ACCELERATED SABOTED RODS SUBJECTED TO LATERAL FORCES

AUTHOR(S): Donald A. Rabern

SUBMITTED TO: 1989 Flash Radiography Topical Symposium, August 15-18, 1989, Rippling River Conference Center, Welches, Oregon

Los Alamos National Laboratory
Los Alamos, New Mexico 87545

AXIALLY ACCELERATED SABOTED RODS SUBJECTED TO LATERAL FORCES

Dr. Donald A. Rabern
Technical Engineering Support, MS G787
Los Alamos National Laboratory
Los Alamos, NM 87544

INTRODUCTION

Considerable effort has been dedicated to ensuring the structural integrity of long rods during axial acceleration, but little work has addressed the subject of lateral acceleration of the sabot/rod package while it is still in-bore. Drysdale (ref. 1) states "Certainly the most pressing unsolved problem facing the projectile designer at the present time does not involve structural integrity directly. Rather it is the development of a methodology which allows the rational design of in-bore configurations so that balloting and sabot separation have a minimal effect on the flight of the subprojectile." Characterization of the response of sabot/rod systems to lateral loading is the next fundamental step to improving sabot designs. Benchmarked analyses and methodology will provide projectile designers with both quantitative and qualitative information to characterize the structural integrity of sabots that are subjected to lateral loads during launch.

A numerical and experimental program was undertaken to determine a method for describing in-bore responses of sabot/rod systems to lateral loads. This program is centered around the M829 saboted long-rod penetrator shown in Fig. 1 (ref. 2) and the 120-mm-diameter smooth-bore launch tube (ref. 3). The philosophy of this study was to use radiographic methods for determining the deflected shapes of the rod and sabot as they traveled down the launch tube, then to compare them with the shapes determined by numerical predictions. With a verified analytical model, the stresses, strains, and displacements may be predicted for the entire system, thus characterizing the structural performance of the sabot/rod system. Experimental methods similar to those used by Lucht (ref. 4) were used to record the distorted shape of the sabot/rod system while it was in the launch tube. Numerical analyses utilized an explicit three-dimensional finite element code with the constitutive and sliding algorithms needed for the dynamic analyses.

The M829 sabot/rod was numerically subjected to three separate launch environments to determine its response to axial and lateral loads. The first launch environment was representative of a launch condition with zero or symmetric lateral loads. This condition was considered to isolate the axial acceleration effects. The second environment was representative of a launch condition with minimal lateral loads. The third was representative of significant lateral loads. These latter two environments occurred when the sabot/rod system was accelerated down a relatively straight tube, which produced minimal lateral loading, and a slightly bent tube, which subjected the sabot/rod system to significant lateral loads. Only the slightly bent tube was used in the experimental portion of the project.

The launch tubes used for the project were 120-mm smooth-bore tubes. The thickness of the wall in the launch tube varied from 2.95 in. to 0.78 in. Reinforcement hoops were located at intervals down the tube. The launch tube was mounted in the launch fixture and acted as a cantilever beam. The two launch tubes chosen for this project were a relatively straight tube and a bent tube. The relatively straight tube is designated by Benet Laboratory as SN104 and the bent tube as SN81. Benet Laboratories inspected each tube for line-of-sight straightness. Their inspection reports are available in a report by S & D Dynamics (ref. 5). The inspection recorded lateral displacement from a datum between the centerline at the aft end of the tube and the centerline at the forward end.

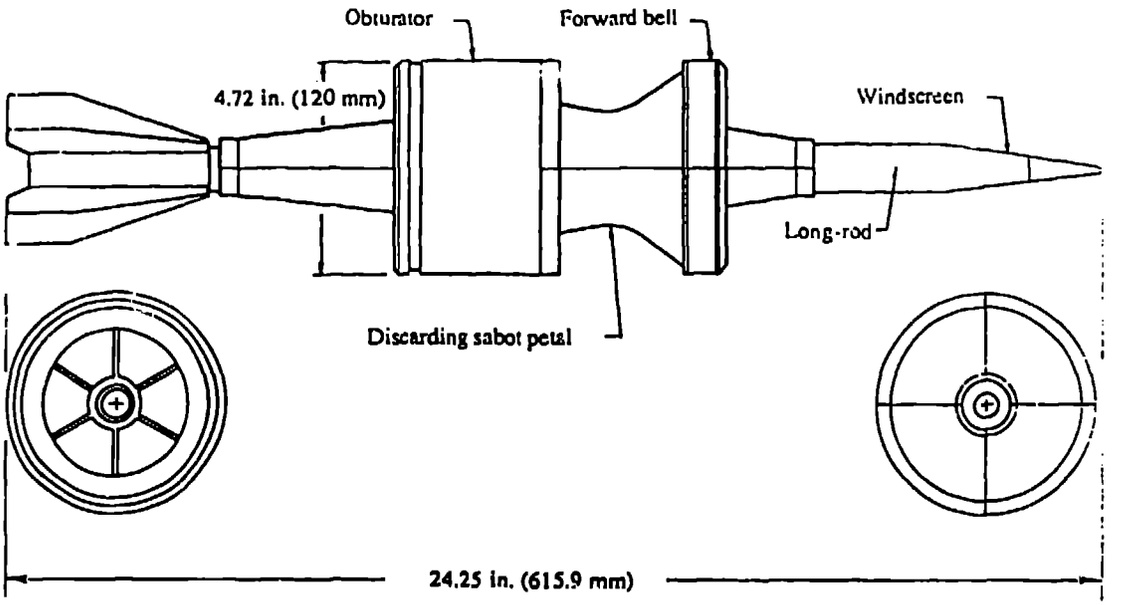

FIGURE 1--Schematic of M829 Sabot/rod.

The tube was modeled with the ABAQUS finite element code (ref. 6) and subjected to the body loads associated with gravity to determine the tube droop. The finite element mesh was generated using the preprocessor PATRAN (ref. 7). The analysis was static, linearly elastic and was performed to determine the tube's shape as a result of gravity and to determine the effect the droop has on the projectile path. The relatively straight (SN104) and bent (SN81) launch tubes are plotted together in Fig. 2. The two tube profiles represent the tube droop and line-of-sight straightness combined for launch tubes SN81 and SN104. These were the initial conditions of the launch tubes prior to launch.

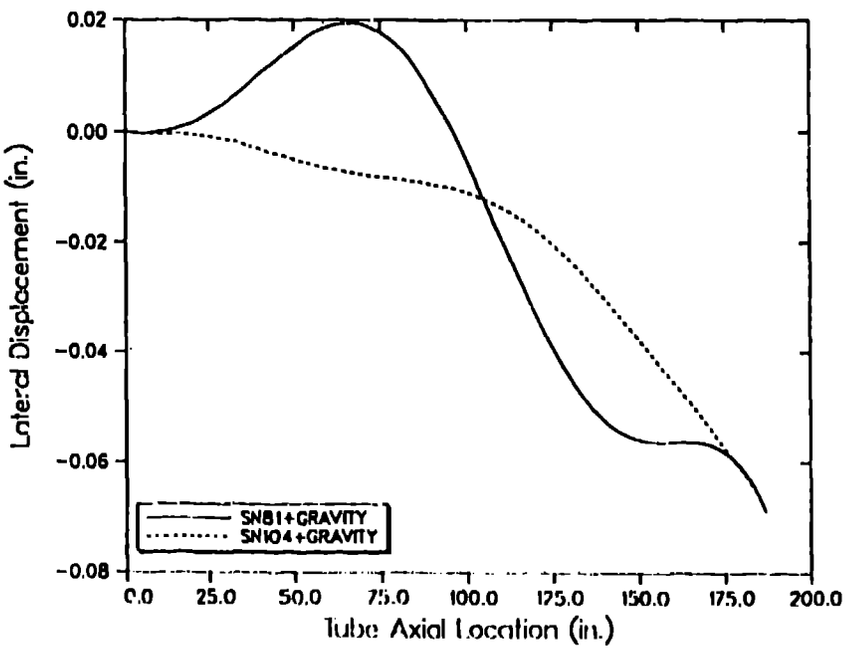

FIGURE 2--Comparison of Lateral Displacement versus Axial Location for Launch Tubes SN81 and SN104.

EXPERIMENTAL WORK

The experimental portion of the research centers around the full-scale testing of the M829 sabot/rod (Fig. 1) in a bent launch tube (Fig. 2). The primary diagnostic tool is a 2.3-MeV x-ray source that is used to record the sabot/rod shape at a known location in the launch tube. For each test performed, the distorted shape was compared with those from previous tests and was used as a benchmark against the numerical predictions. Two pairs of orthogonal x-ray units were used to record launch tube exit velocity, sabot separation, and rod straightness.

The test range consists of the sabot/rod launch facility, instrumentation, and sabot stripper. A photograph of the instrumentation and launch facility is shown in Fig. 3. A schematic of the facility is shown in Fig. 4. Also shown in the figure are locations of the x-ray head and triggers, with station location highlighted for clarity. The following is a narrative of events by station.

- **STATION A:** The propellant is ignited with an electrical charge, pressure builds in the breech, and the sabot/rod begins to travel down the tube.

- **STATION B:** Evacuator ports are located at station B. Two capped pin switches are inserted into the evacuator ports. When the forward bell of the sabot hits the pins, the signal is recorded and used as a timing mark to signal the x-ray units. A time interval meter triggers the 2.3 MeV x-ray tube to fire approximately 0.63 ms after the pin switch is tripped. The time varies, depending on the tube's axial location for the experiment.

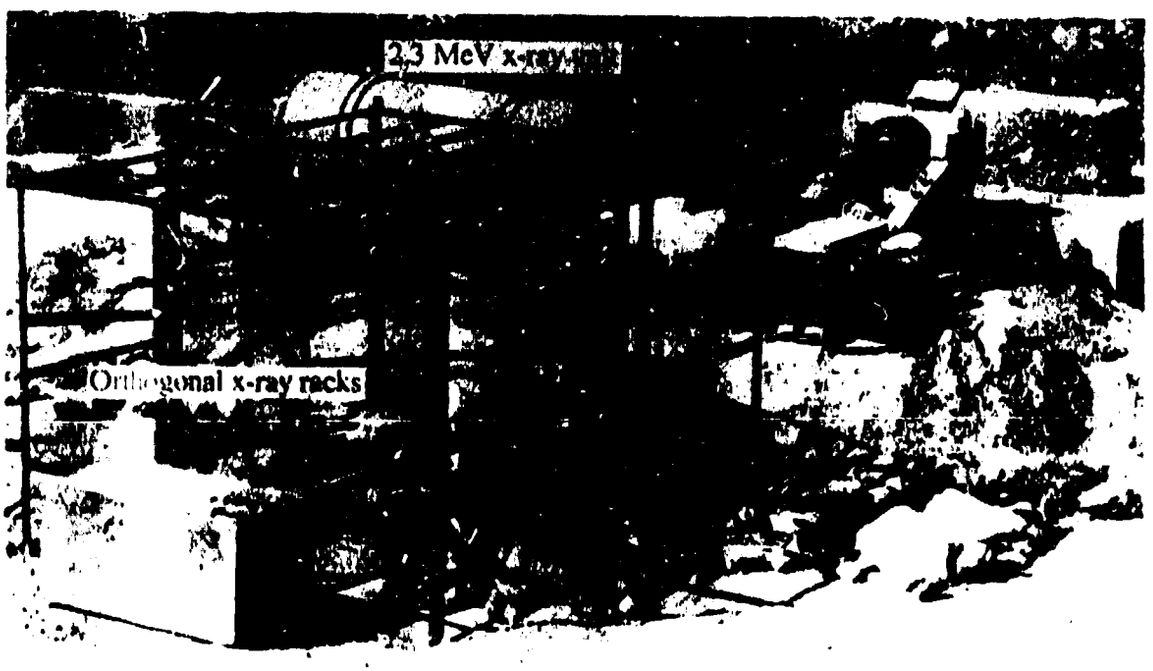

Figure 3. Test Range.

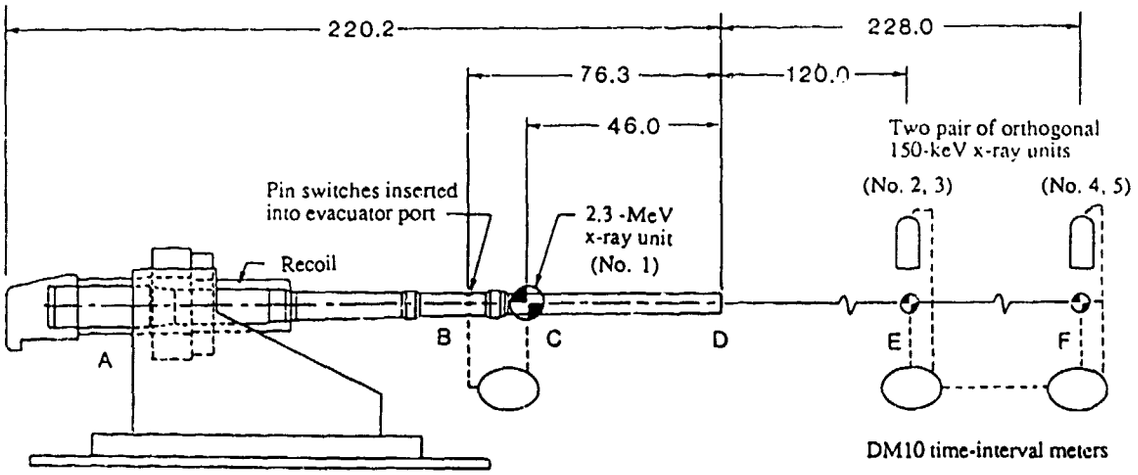

Notes:

1) A, B, C,... F designate station locations.

2) Dimensions are in inches from muzzle.

Figure 4. Range Schematic.

- **STATION C:** The trigger from the time interval meter triggers the 2.3-MeV x-ray unit, and the unit pulses, recording the sabot/rod image on the shielded film pack opposite the x-ray tube. The location was chosen from code predictions of where the maximum lateral displacement should occur.

- **STATION D:** The sabot/rod system exits the launch tube and aerodynamic forces begin to strip the sabot petals from the rod.

- **STATION E:** The sabot petals begin to separate, and a pair of orthogonal 150-keV x-ray tubes pulse. This records the rod and sabot images on the film packs after a 3.08-ms delay from the pin switches.

- **STATION F:** A third interval meter counts approximately 4.72 ms from the pin switch, then pulses the second set of orthogonal x-ray tubes. This records the image of the sabot and rod.

The major diagnostic tool in the experiment is the 2.3-MeV x-ray unit. For the application of in-bore radiography, the unit is slightly underpowered. The system is a standard 2.3-MeV Hewlett-Packard flash x-ray unit with a rated dose of 125 mR at 6.56 ft and a spot size diameter of 0.196 in. Its rated pulse width is 25 ns. The x-ray diode was positioned approximately 67 in. from the centerline of the launch tube and was centered at Station C. Lead shields were used to prevent fog, to enhance resolution, and to provide contrast. A 4-in. lead wall was constructed in front of the x-ray tube with a 0.5-in. by 5-in. collimation hole to prevent scatter. A 0.125-in. lead sheet was wrapped around the x-ray tube to prevent radial scatter and a 0.25-in. lead sheet was placed on the table to prevent scatter from reflecting off the table. A lead shielding box was designed and built to prevent scatter from the launch tube and to completely enclose the film pack, except through the viewing area. The shielding techniques used made it easy to reassemble the package between tests and were instrumental in obtaining quality radiographs. Shown in Fig. 5 are the x-ray tube, launch tube, x-ray and film shields, and the 150-keV orthogonal racks. The insufficient x-ray intensity was overcome by using multiple layers of film in the x-ray cassette.

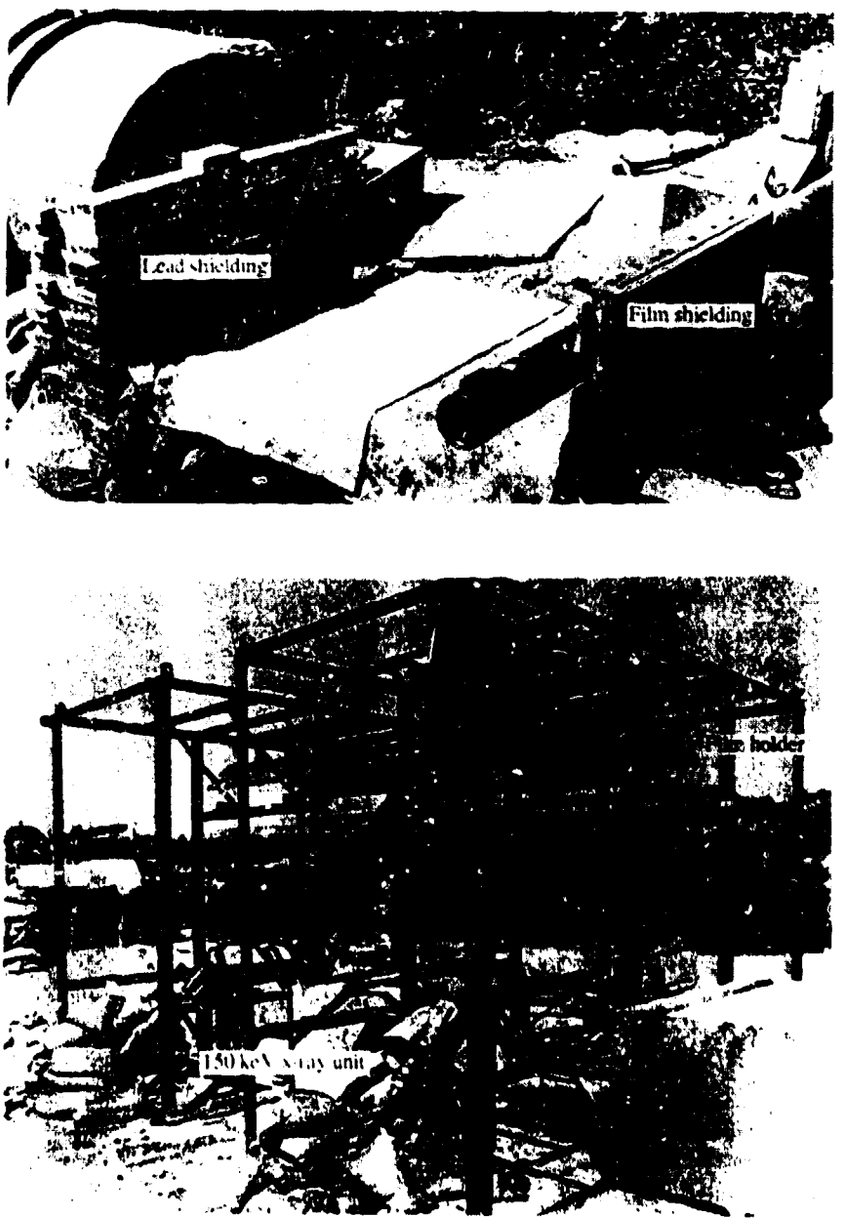

Figure 5. 2.3-MeV and 150-keV Flash X-ray Setups.

Dupont Cronex industrial NDT57 and NDT9 intensifier screens were used in the screen/film/screen sets. Two sets were used in the film pack. They were indexed with pins to provide alignment. A bladder placed around the entire film pack was evacuated to ensure good screen-to-film contact. After development, the films were superimposed to improve effective exposure and signal-to-noise (S/N) ratio. The two separate films were digitized on a scanning microdensitometer, then their results were averaged. A reconstructed image, in which density gradients were removed and contrast was optimized, was used to bring out resolution and features required to determine the rod's distorted shape.

Three capped-pin switches (ref. 8) and a logic circuit were used to trigger the x-ray unit. This redundancy ensured proper triggering of the x-ray unit. Capped pins were required to eliminate the possibility of premature tripping that could result from hot ionized gas leaking past the obturator ring and the shorting of an uncapped switch. Two pairs of orthogonal, 150-keV flash x-ray units were set up in a racks down range from the launch tube centered on the shot line at Stations E (Numbers 2 and 3) and F (Numbers 4 and 5) (Figs. 4 and 5). These were located so that the diode of the x-ray tube was approximately 72 in. from the shot line. The film cassette was an additional 24 in. from the shot line, for a distance of 96 in. between the diode and film pack.

Radiographs from X-ray units 2 through 5 were digitized to determine rod straightness. The upper and lower rod edges were digitized on a personal computer and recorded. Results were transmitted to a Cray computer and manipulated with the program TDAP (ref. 9). The upper and lower edges were averaged to produce the rod centerline and then a third-order polynomial fit was done to determine the rod's deformed shape along its centerline The results of the data analyses showed the rod's deformed shapes at two orthogonal stations for each test.

Radiographs from the 2.3-MeV x-ray unit look similar between tests. Postprocessing of the image is required to obtain a quantitative deformation pattern in the rod. A typical radiograph of the M829 sabot/rod system taken with the 2.3 MeV x-ray unit (Station C) and the enhanced in-bore radiograph are shown in Fig. 6. Radiographs from the 150-keV x-ray units (Stations E and F) are shown in Fig. 7. In the 2.3 MeV x-ray the U.75Ti rod and details, such as thread form and rod taper, are clearly visible. The fins, sabot, and windscreen are easily discernible. Although fog begins to cloud the image near the internal diameter of the launch tube, the rod details are adequate for postprocessing. This radiograph was taken 46 in. from the muzzzle and the sabot/rod velocity was approximately 1.55 km/s.

The beginning of sabot separation shown in the top image of Fig. 7 was taken with X-ray unit Number 2; the lower image, taken with X-ray unit Number 5, shows the sabot parts as they continue to separate from the rod. The rod had an approximate velocity of 1.66 km/s when the radiographs were taken. The line in the center of both images is caused by a film seam.

The M829 deformed rod shapes calculated from in-bore radiographic results in Tests 1, 2, and 3 are shown in Fig. 8. The deformed rod shapes are plotted at three axial locations. The skew in the data does not indicate yaw or lack of yaw, but the indexing method used. The ordinate is exaggerated, compared with the abcissa, to show the lateral displacement more clearly. The top plot shows the deformation of the rod at an axial launch tube location 66.3 in. from the fins of the rod to the muzzle of the launch tube (Test Number 2). Most of the lateral displacement is in the tip of the rod (0.048 in.) and is measured from the center of gravity of the rod. The tail lateral displacement is -0.011 in. at this location in the launch tube. The middle plot shows the distorted shape 58.2 in. from the muzzle (Test Number 1). The tip lateral displacement is now 0.043 in. and the tail displacement is now 0.007 in. The bottom plot shows the distorted shape 51.7 in. from the muzzle (Test Number 3). The tip lateral displacement is now 0.025 in , and the tail displacement has changed to 0.036 in. The results show the rod's deformed shapes at three axial locations in the launch tube. The length of the film and the location of the 2.3-MeV x-ray unit made it impossible to perform tests to determine the entire deformation cycle of the rod.

Figure 6. Typical In-Bore Radiograph and Corresponding Enhanced Radiograph.

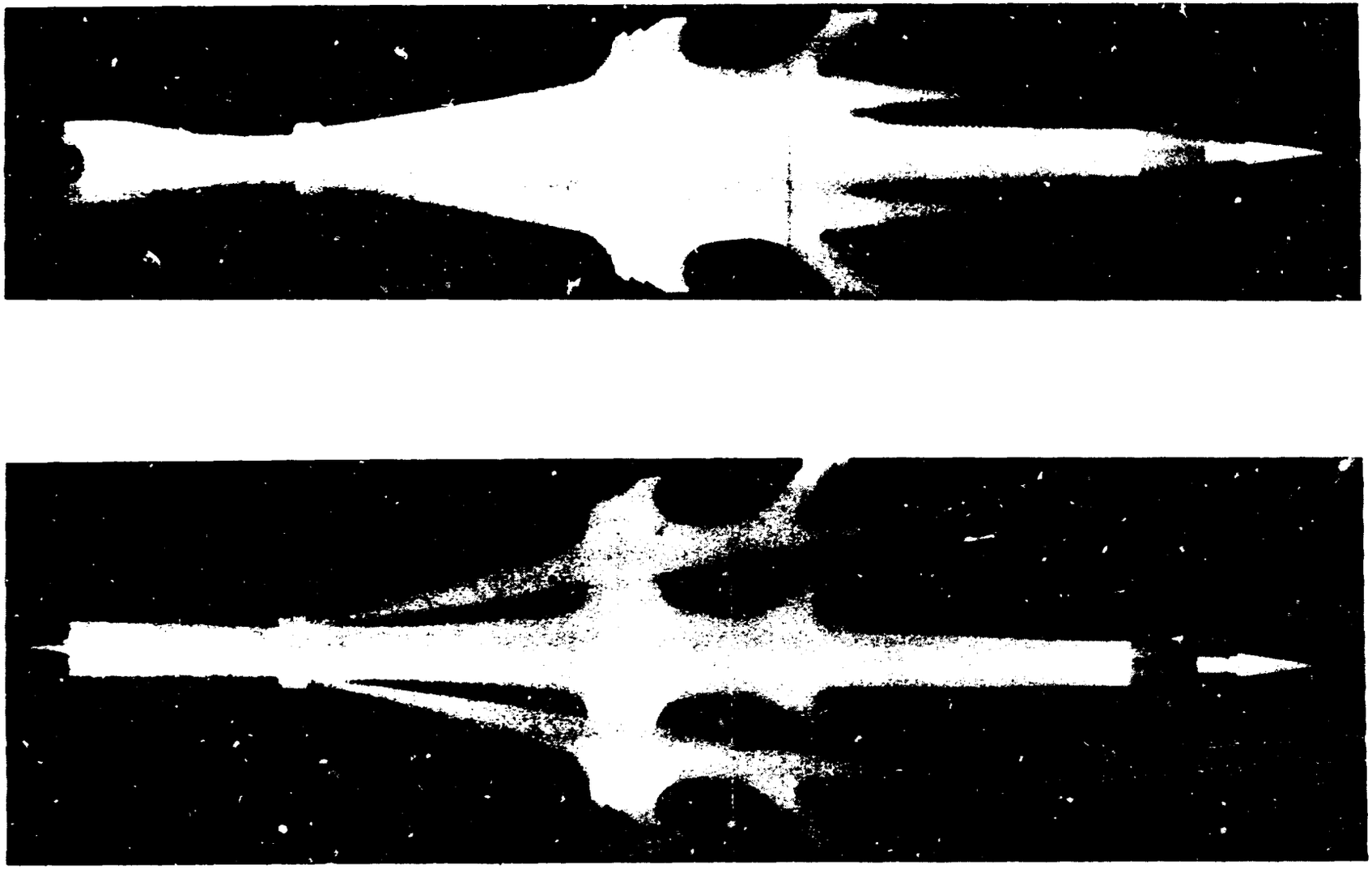

Figure 7. Typical Radiographs During Sabot Separation.

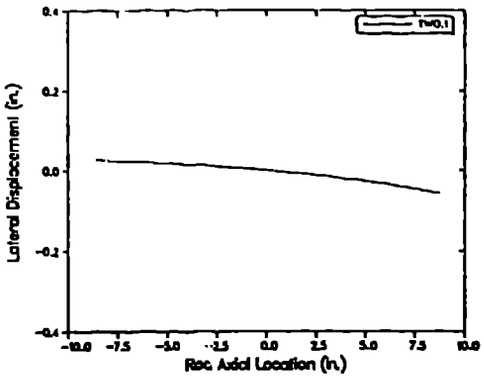

Deformed rod 66 in. from launch tube muzzle.

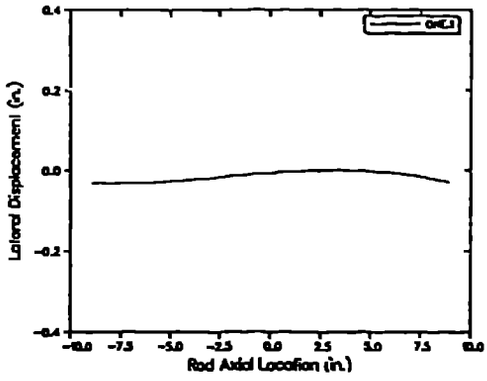

Deformed rod 58 in. from launch tube muzzle.

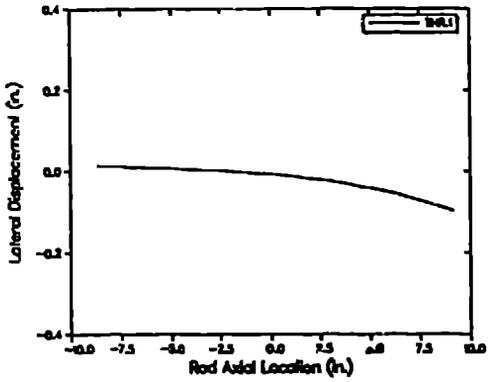

Deformed rod 52 in. from launch tube muzzle.

Figure 8. M829 In-bore Rod Deformed Shapes.

NUMERICAL MODELING

The sabot/rod systems and their launch environments were modeled numerically to describe in detail the structural behavior of each system as it travels down each of the launch tubes. The numerical modeling was performed to predict the stress environment and the response of the sabot/rod system. The data obtained were used to compare the structural integrity of the three separate sabot designs. The M829 sabot/rod was modeled in three different launch tubes. The first launch tube was perfectly straight and was modeled to remove the effects of lateral loading on the sabot/rod system. The second launch tube, SN104, was modeled to observe the effect of minimal lateral loading on the sabot/rod system. The third launch tube, SN81, was modeled to observe the effects of significant lateral loads on the system. DYNA3D (ref.10), an explicit finite element code, was selected for the analyses. This code has traditionally been used for dynamic transient analysis involving impact and contact surfaces. A 180-degree model was generated, rather thar a full 360-degree system. Appropriate boundary conditions were applied on the symmetry plane. The tube environment selected showed little motion normal to the constrained surface and was assessed to have small effects on the analysis results. With the 180-degree model,

the problem size was cut significantly over a full 360-degree model. Shown in Fig. 9 is the M829 sabot/rod mesh in launch tube SN81 at time zero.

Results from Tests 1, 2, and 3 were compared with results from the numerical analyses. These tests used the M829 sabot/rod in launch tube SN81. The deformed shape of the rod at the centerline was calculated for each test and was plotted at the same displacement scale factor as was used in the numerical analyses. These results are superimposed on the deformed finite element mesh at the corresponding axial locations in the launch tube. Shown in Fig. 10 are the comparisons at three separate locations. The launch tube's axial locations, rather than times, were chosen to take into account the small differences in velocity between the physical testing and the numerical analyses. The numerical analyses were performed with an exit velocity of 1.65 km/s, where the physical experiments showed velocities between 1.67 and 1.69 km/s. Thus, axial location was used to compare the results. As indicated in Fig. 10 the deformed pattern from testing closely matches the numerical analyses. The top comparison shows the rod 66 in. from the launch tube muzzle. The measurement is made from the tail fins of the rod. The middle comparison shows the rod 58 in. from the muzzle, and the bottom comparison shows it 51 in. from the muzzle. The data show that the numerical analysis deformation cycle is slightly faster than shown in the physical tests. The effect is small. The general shape of both tests and numerical analyses agree well. Table I is a summary of the tip and tail displacements from both the numerical analyses and the physical tests.

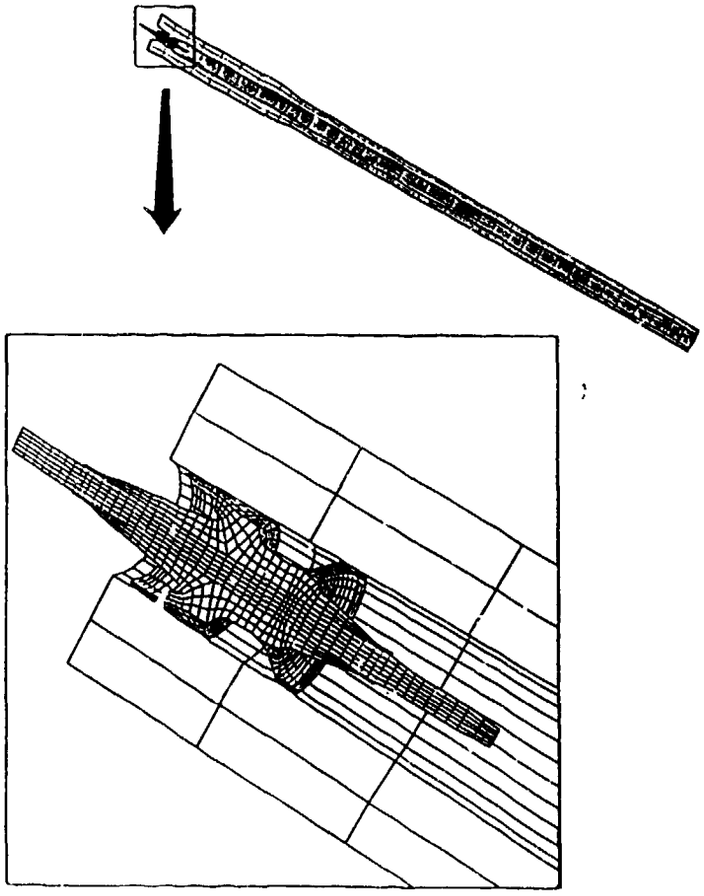

Figure 9. Finite Element Mesh of Sabot/rod System and Launch Tube.

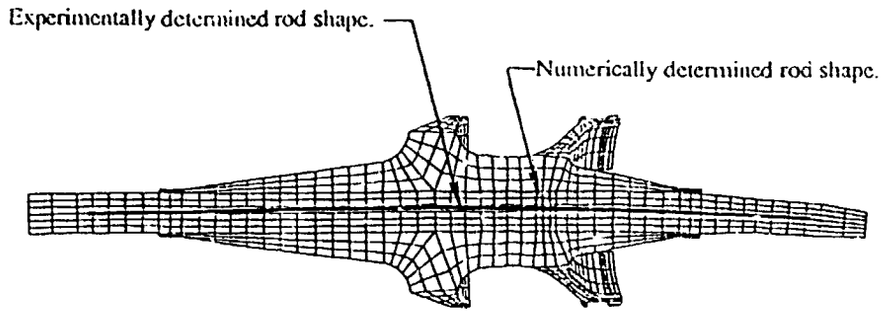

Deformed rod 66 in. from launch tube muzzle.

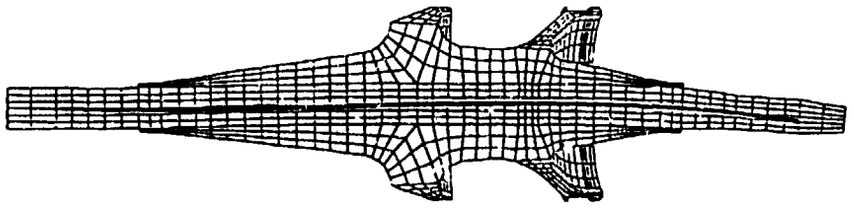

Deformed rod 58 in. from launch tube muzzle.

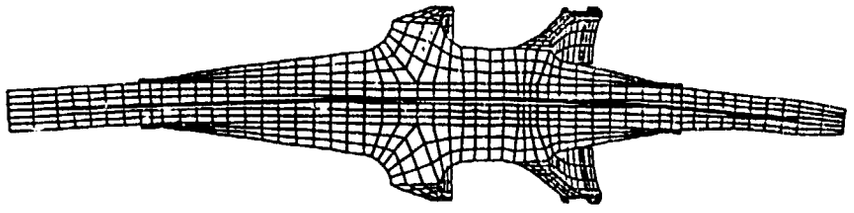

Deformed rod 52 in. from launch tube muzzle.

Figure 10. Comparison of Numerically and Experimentally Determined Rod Deformed Shapes.

Table I. A Comparison of Tip and Tail Displacements: Experimental Testing vs Numerical Analyses of the M829 Sabot/rod in Launch Tube SN81

	Axial Location (in.)		
	66	58	51
Numerical Tip Displacement	0.042	0.037	0.018
Experimental Tip Displacement	0.048	0.043	0.025
Numerical Tail Displacement	-0.016	0.004	0.032
Experimental Tail Displacement	-0.011	0.007	0.036

With a verified model, stresses, strains, and displacements may be extracted from the numerical analyses to determine the structural response of the system in the tube. The data are voluminous, so only a very cursory view is presented here. The tip and tail lateral displacement with respect to the center of gravity of the rod is shown in Fig. 11 for the M829 sabot/rod as it transits launch tube SN81. The von Mises stress contours are plotted on the deformed mesh just prior to exiting the launch tube in Fig. 12. The distorted geometry is shown for the sabot/rod in all three launch environments. The perfectly straight launch environment is used to isolate the stresses caused by the axial load environment. Table II shows the peak von Mises stresses that occur in each launch environment at seven selected times during the launch process.

The results indicate that for launch tube SN81 the lateral loadings do not significantly affect the sabot/rod until the velocity has increased in the latter stages of launch. At this point the effect, compared with that of the perfectly straight launch tube (PS), develops as much as 296% higher stresses because of the lateral stress environment.

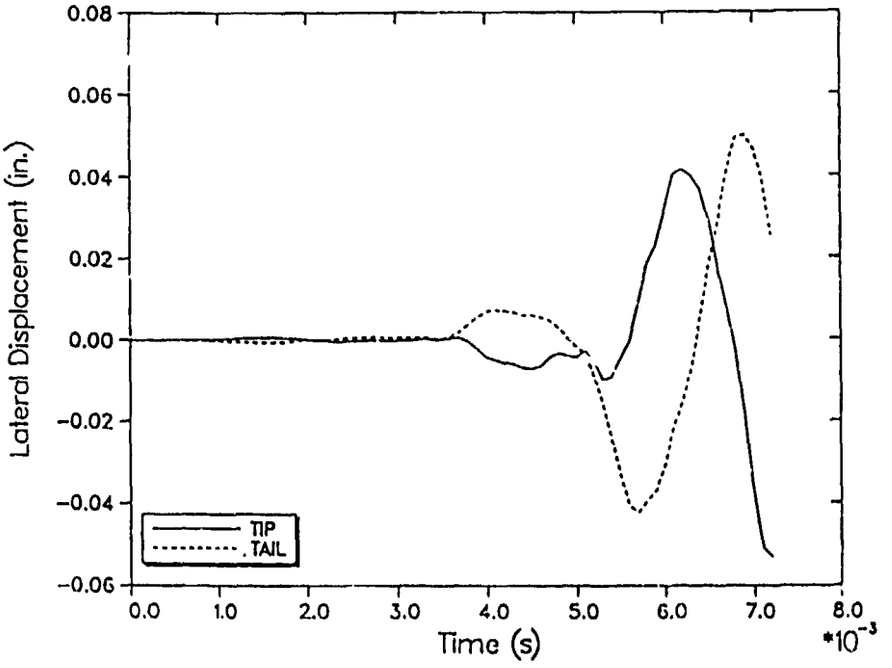

Figure 11. The M829 Sabot/rod Tip and Tail Deflections versus Time with Rigid Body Displacements Removed as it Transits Launch Tube SN81.

Table II. Maximum von Mises Stress (ksi) for Three Launch Environments at Seven Selected Times

	Times (s)						
Launch Tube	0.0034	0.0039	0.0047	0.0053	0.0063	0.0069	0.0072
SN81	82	88	75	74	67	42	74
SN104	82	88	76	60	52	35	37
PS	82	88	76	63	37	29	25

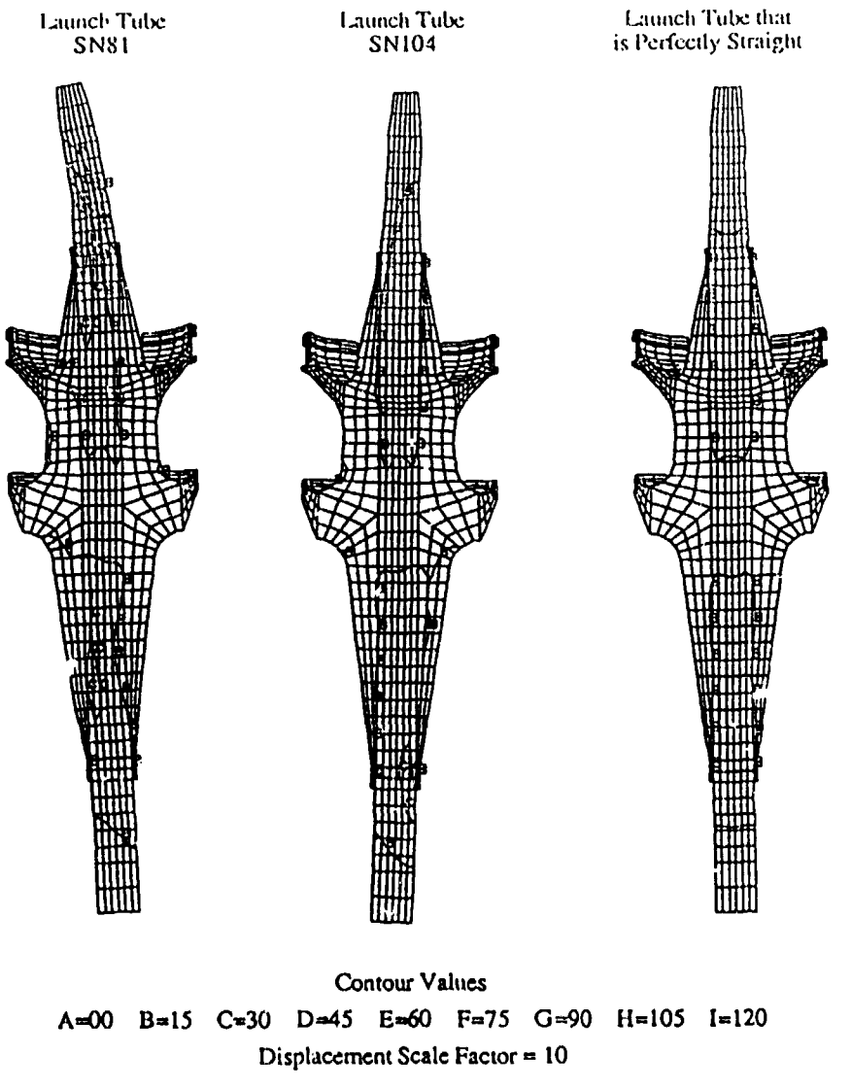

Figure 12. The von Mises Stress Contours (ksi) on the Distorted Geometry at 0.0072 s for the M829 Sabot/rod System in Launch Tube SN81 and Launch Tube SN104 and in a Launch Tube that is Perfectly Straight.

SUMMARY AND CONCLUSIONS

With the setup and the numerical and experimental components completed, several conclusions can be made regarding the methodology employed for the project. The original intent of the project was to establish a methodology that accurately describes the structural behavior of a sabot/rod system subjected to in-bore lateral loading. To accomplish this, experimental and numerical methods were employed that provided the detail required to make the necessary comparisons between launch environments. X-ray enhancement techniques and large computers are necessary technologies for conducting a successful analysis. The experimental and numerical portions of the method complement one another by obtaining the independent data required to fully characterize the sabot/rod structural response. The experiments provide a benchmark for the numerical studies and subsequent information during sabot separation.

The numerical models provide detailed information about stress, strain, and displacement histories that are not available from the experiments. Considerations and conclusions about the numerical models used are noted here. The combination of the numerical and experimental methods constitute the methodology employed in this analysis. The most significant conclusion about the methodology employed would be that the combination of numerical modeling and full-scale experiments provides sufficient information to characterize the in-bore structural behavior of sabot/rod systems. To be successful however, a thorough understanding of the initial conditions, launch environment, system geometry, and loading conditions is essential.

ACKNOWLEDGMENTS

The author wishes to acknowledge the funding provided by the United States Department of Army, the Department of Energy, and the Ballistic Research Laboratory. He also wishes to recognize the contributions of B. P. Burns, W. Biems, K. Fehsel, J. W. Straight, R. A. Lucht, R. E. Garcia, M. Avilla, W. A. Cook, G. C. Langner, R. K. London, J. P. Bradley, M. A. Fletcher, W. D. Birchler, and D. A. Marshall. This was a joint program between groups WX-4 and M-8, both of Los Alamos National Laboratory.

REFERENCES

[1] Drysdale, W. H., "Design of Kinetic Energy Projectiles for Structural Integrity," US Army Ballistic Research Laboratory technical report ARBRL-TR-02365, Aberdeen, MD (1981).
[2] Ballistic Research Laboratory, "Sabot Annular Grooves," Drawing No. 12525543, Aberdeen, MD (October 19, 1981).
[3] Benet Laboratory, "Tube," Drawing No. 12529794, Watertown, MA (December 3, 1979).
[4] Lucht, R. A., "In-Bore Radiography for Large-Caliber Guns," in Proceedings from the Tenth International Symposium on Ballistics, San Diego, CA (October 1987).
[5] S & D Dynamics, "Dynamic Analysis of the 120 mm Tank Gun," Contract Report BRL CR-576, Aberdeen, MD (1987).
[6] Hibbett, Karlson, and Sorenson Inc., ABAQUS User's Manual Version 4.5a, Providence, RI (1985).
[7] PDA Engineering, PATRAN Plus User's Manual, PDA Engineering, Costa Mesa, CA (1987).
[8] DYNASEN Inc., Shock Pressure Sensors and Impact Facilities, Goleta, CA (1985).
[9] Birchler, W. D., and Wheat, B. M., "TDAP - Test Data Analysis Program," Los Alamos National Laboratory user manual (in preparation), Los Alamos, NM (1989).
[10] Hallquist, J. O., and Benson D. J., "DYNA3D User's Manual (Nonlinear Dynamic Analysis of Structures in Three-Dimensions)," Lawrence Livermore National Laboratory report UCID-19592 Rev. 3, Livermore, CA (1987).